

Brillouin Light Scattering Analysis of Ultra Short Microwave Pulse Formation Processes in Yttrium Iron Garnet Films

C. MATHIEU, V. T. SYNOGACH, and C. E. PATTON

*Department of Physics, Colorado State University
Fort Collins, Colorado 80523, USA*

Abstract - Wave vector selective Brillouin light scattering has been used to observe directly the half frequency parametric magnons in the three magnon splitting process responsible for ultra short microwave pulse formation from nonlinear magnetostatic surface waves in yttrium iron garnet films. The frequencies and wave vectors of the relevant spin waves and threshold powers for the onset of these processes were quantitatively determined.

INTRODUCTION

Recently, the generation of extremely short microwave pulses as narrow as 2 ns from relatively long magnetostatic surface wave (MSSW) input pulses in yttrium iron garnet films (YIG) at high power has been demonstrated [1]. These short pulses were obtained with a long and narrow YIG film strip in a standard magnetostatic wave delay line structure. This ultra short pulse generation required a frequency below 3.3 GHz, the cut off for three magnon splitting processes in YIG [2].

The model proposed in [1] to explain the pulse formation involves MSSW magnons which split into two approximately half frequency dipole exchange spin wave (DESW) modes with wave vectors on the order of 10^4 rad/cm. Brillouin light scattering (BLS) techniques have now been used to analyze the generation of these DESW excitations in the above process. The frequencies and wave numbers for these magnons are as expected from the model. The data also give specific threshold power levels for the different DESW magnon pairs involved in the three magnon process.

EXPERIMENT

The microwave measurements were performed in the same way as in [3]. The experiments utilized a microstrip antenna structure with a 2 mm wide, $8.7 \mu\text{m}$ thick YIG strip with a nominal length of 12 mm. The film was magnetized in-plane by a static magnetic field perpendicular to the long side of the strip and the MSSW propagation direction. The structure consisted of one fixed and one movable $50 \mu\text{m}$ wide microstrip antenna placed perpendicular to the YIG strip. The fixed antenna was used for input and the movable antenna was used for

output. Data were obtained for MSSW carrier frequencies above as well as below the 3.3 GHz three magnon cut off. The detailed BLS three magnon experiments were done for an MSSW frequency f_s of 2.6 GHz. The input pulse width was about 100 ns. The duty cycle of the input signal was kept below 5 % in order to avoid heating effects.

The BLS measurements were made with an automated multipass tandem Fabry-Pérot interferometer in forward scattering geometry [4]. The wave vector selective measurements were based on the technique given in [5]. Linearly polarized light at 514.5 nm wavelength from an Ar^+ ion laser at a 15-20 mW power level is focused by a 50 cm focal length lens onto the YIG film at normal incidence. The low power is needed to eliminate heating effects. The YIG sample was mounted on a 3-axis stepper motor controlled translation stage in order to move the probe beam to different points on the sample. The direct transmitted beam through the semi-transparent film and the forward scattered light are collected by a standard photographic lens. Wave vector selective scattering data were obtained from sequences of measurements for different sized on-axis circular apertures placed after the collection lens. With a precise match-up of the aperture center to the direct beam axis, it was possible to select wave numbers from zero to upper limit k_{max} values up to $4H10^4$ rad/cm. See [5] for further details of the technique.

RESULTS

The most important result from the microwave experiments in [1] was the significant pulse narrowing which occurred for MSSW pulses at high power when the carrier frequency was below 3.3 GHz. Figure 1 shows the typical pulse narrowing microwave response as a function

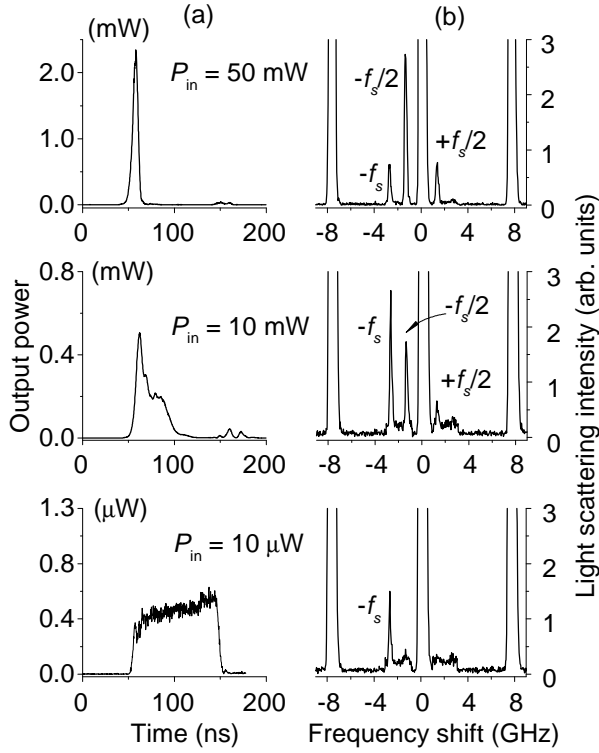


Fig.1(a) shows microwave output power vs. time profiles and (b) corresponding Brillouin light scattering spectra. The pairs of graphs from bottom to top are for increasing values of the input peak power P_{in} , as indicated.

of input power (a) and a corresponding series of BLS spectra (b). For these specific data, the input pulse width was 100 ns, the signal frequency was 2.6 GHz, and the static field was about 340 Oe. As in [1], similar microwave results are obtained for a range of pulse widths and frequencies. The BLS set up contained no wave vector selective elements for these measurements.

For the input power level P_{in} set to a low value of 10 μW , as in the lower left graph, the output power simply maps the 100 ns long input pulse. As P_{in} is increased, one first sees a change in the output pulse shape at P_{in} values of about 100 μW , as shown in the middle left graph. For this range of powers, the trailing edge of the pulse begins to drop. A further increase in power causes a total collapse of the output pulse, except for a very narrow pulse at the leading edge of the original pulse. As shown in the top left graph for $P_{in} = 50 \text{ mW}$, the output pulse has narrowed to 5 ns. Pulses as short as 2 ns could be generated for slightly thicker YIG films with optimal input power settings and antenna separations.

The BLS spectra in (b) show that there are also significant changes in the magnetic excitations in the film

as the input power is changed. Note that the spectra show dominant central and ghost elastic peaks at zero frequency and at $\pm 7.5 \text{ GHz}$. The region of interest here is for frequencies between about 0.9 and 3.3 GHz.

At the lowest power, $P_{in} \approx 10 \mu\text{W}$, the BLS spectrum contains only a single peak at $-f_s$. Note that this strong peak is on one side of the spectrum only. One may associate this single strong peak with the fact that the magnons are from the externally excited MSSW signal. Extended measurement times also lead to a weak peak at $+f_s$ [6]. The middle right graph shows the effect of increased power. As P_{in} increases, one observes the emergence of additional peaks in the spectrum at approximately $\pm f_s/2$. Note that there are now peaks on both sides of the central peak. These $\pm f_s/2$ peaks are signatures that the nonlinear generation of the half frequency DESW magnons has commenced. Finally, the top right graph shows that at $P_{in} = 50 \text{ mW}$, just as one obtains ultra short pulse formation, the BLS peaks at $\pm f_s/2$ increase rapidly in strength and become much larger than the original f_s peak.

The results in Fig. 1 provide direct evidence for the parametric excitation of half frequency spin waves as part of the process which leads to the ultra short pulses. These data show that the technique provides an extremely sensitive way to detect the relevant magnons and actually observe the onset of the nonlinear interactions, which produce these magnons.

Detailed measurements over the active region of the YIG film between antennas show that the strength of the parametric $f_s/2$ magnon signal depends on the spatial position, the direction and size of the magnon wave vector, and the power. The full ensemble of these results is beyond the scope of this paper and will be presented elsewhere. The proof that three magnon splitting is the process responsible for ultra short pulse formation in YIG films, however, can be readily demonstrated from selected results on the wave number dependence of the BLS peak response at $\pm f_s/2$ for different powers. These results are presented below.

According to the model in [1], dipole exchange spin wave (DESW) excitations close to $f_s/2$ are parametrically pumped by the low wave number input MSSW signal. The MSSW signal has a wave vector \mathbf{k} in the propagation direction and the DESW \mathbf{k} -values are in the film plane and nearly perpendicular to this direction. Through three magnon confluence processes, these DESW

magnons then combine to produce the wide band spectrum of spin waves centered at f_s which leads to the short pulses.

Wave vector selective BLS measurements have provided a direct way to probe the details of the above processes. Data were obtained with the wave vector selective diaphragm in place and set to different diameters to yield different cut-off wave number k_{\max} limits. For diaphragm diameters below 1 mm, the BLS peak signal at $-f_s$ remained unchanged but the peaks at $\pm f_s/2$ were eliminated. This diameter, therefore, defines a k_{\max} limit of about 1250 rad/cm for the wave number distribution for the MSSW signal. This cut off is consistent with antenna coupling considerations and with the spread in k values expected for the MSSW band of excitations, which make up the narrow pulse at high power.

The threshold power levels for the parametric excitation of the DESW magnons were obtained from further data on the $-f_s/2$ BLS peak intensities as a function of diaphragm diameter and the corresponding k_{\max} wave number limit. Figure 2 shows two representative sets of data on scattering signal vs. k_{\max} for the $-f_s/2$ peak. For each P_{in} value, one obtains a threshold response for the onset of the DESW half frequency signal. There are distinct step increases in the signal at k_{\max} values of $12\text{H}10^3$ and $21\text{H}10^3$ rad/cm for P_{in} values of 32 mW and $64 \mu\text{W}$, respectively.

The threshold effect shown in Fig. 2 correlates with the allowed DESW wave numbers for three magnon splitting expected from the dispersion curves and energy and momentum conservation considerations. Figure 3 shows the three lowest DESW dispersion branches calculated from [7] for the experimental parameters. The solid circles

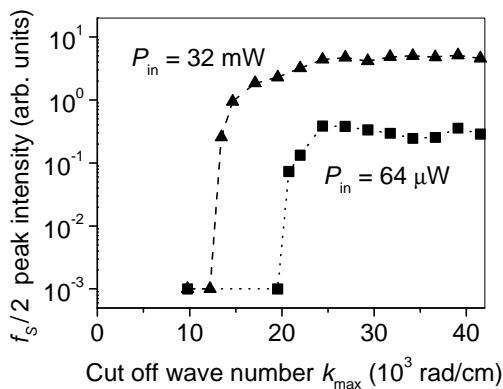


Fig.2. Integrated BLS intensity for the $-f_s/2$ peak as a function of the diaphragm cut-off wave number k_{\max} for two input power P_{in} levels, as indicated.

indicate the two lowest k pairs of magnons for which the splitting is allowed. Note that for each pair, one actually has plus and minus k values for momentum conservation. The k values of $11.6\text{H}10^3$ and $20.2\text{H}10^3$ rad/cm for these mode pairs are in good agreement with the threshold k_{\max} values from the data. The results in Fig. 2 also indicate that parametric magnons with higher k values, which derive from higher order DESW branches, have much lower power thresholds.

ACKNOWLEDGEMENTS

This work was sponsored in part by the National Science Foundation (USA), Grant DMR-9801649 and the U. S. Army Research Office, Grant DAAG55-98-1-0430.

REFERENCES

- [1] V. T. Synogach, Y. K. Fetisov, C. Mathieu, and C. E. Patton, submitted to Phys. Rev. Lett. (2000).
- [2] A. M. Mednikov, Fiz. Tverd. Tela (Leningrad) **23**, 242 (1981) [Sov. Phys. Solid State **23**, 136 (1981)].
- [3] N. G. Kovshikov, B. A. Kalinikos, E. S. Wright, and J. M. Nash, Phys. Rev. **B 54**, 15210 (1996).
- [4] B. Hillebrands, Rev. Sci. Instr. **70**, 1589 (1999).
- [5] G. Srinivasan, C. E. Patton, and P. R. Emtage, J. Appl. Phys. **61**, 2318 (1987).
- [6] To the knowledge of the authors, up to now there has been no satisfactory explanation for the Stokes anti-Stokes asymmetry usually observed in this kind of experiments.
- [7] B. A. Kalinikos, Sov. Phys. J. **24**, 718 (1981).

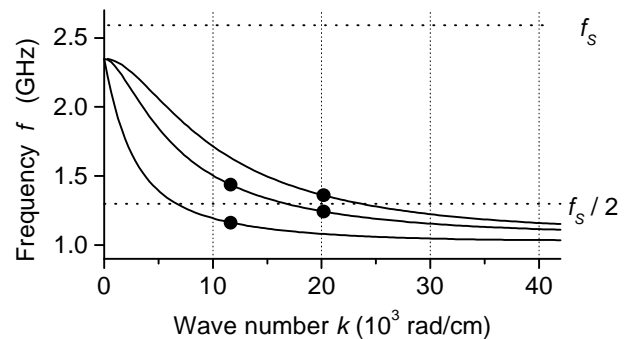


Fig. 3. Dispersion diagram of spin wave frequency f_k vs. wave number k with the lowest three branches of the DESW dispersion for an in-plane magnetized $8.7 \mu\text{m}$ thick YIG film at a field of 340 Oe. The solid circles indicate the allowed pairs of DESW modes for splitting.